

Electrical Conductivity and Viscosity of Aqueous NaCl Solutions with Dissolved CO₂

Marc Fleury* and Hervé Deschamps

Institut Français du Pétrole (IFP), Petrophysics Department, 92852 Rueil-Malmaison, France

The effect of dissolved CO₂ on the electrical conductivity and viscosity of three NaCl solutions covering the range of salinity usually encountered in potential CO₂ storage geological formations has been studied. At a constant temperature of 35 °C, the variations of conductivity and viscosity are proportional to the mole fraction of dissolved CO₂. For viscosity, our data are in agreement with previous observations. The observed variations are small and are at maximum on the order of 10 %. The variations of conductivity and viscosity as a function of temperature up to 100 °C are not modified by the presence of CO₂, and we suggest using the empirical Arps model. A simple model is proposed to take into account the small modifications of conductivity and viscosity as a function of the dissolved CO₂ mole fraction and temperature.

Introduction

With the perspective of long-term CO₂ storage, thermodynamic data are necessary for the simulations of CO₂ injection in aquifers of depleted oil reservoirs. We focus here on the determination of the resistivity and viscosity of aqueous NaCl solutions with dissolved CO₂. It is well known that dissolved CO₂ slightly increases the water density.¹ On the basis of the density variation (on the order of 1 %), the influence of dissolved CO₂ on viscosity appears to be negligible. However, Bando et al.² recently measured the viscosity of CO₂-saturated brines and found a significant increase in viscosity with increasing mole fraction of dissolved CO₂. For resistivity, no data are available to our knowledge.

Water viscosity is an important quantity for predicting convection in thick geological storage units. Indeed, when injecting CO₂, the plume has the tendency to flow upward. However, a small amount of CO₂ will dissolve into the water; under the influence of the small density difference, that water has the tendency to flow downward. This flow is therefore driven by density difference, and its time scale is controlled by viscosity effect.

Brine conductivity with dissolved CO₂ is also of interest in the context of electromagnetic monitoring and logging techniques. Whatever the process used, these techniques rely on the contrast between a conductive phase (brine) and a nonconducting phase (hydrocarbon, CO₂). It is therefore useful to determine fully the influence of dissolved CO₂ on ionic conductivity. We can expect two opposite effects: viscosity may decrease conductivity, whereas dissociation may increase conductivity.

We present the simultaneous measurements of the variation of conductivity and viscosity for three NaCl brines of salinity (20, 80, and 160) g·L⁻¹, respectively ((0.342, 1.369, and 2.738) mol·L⁻¹). The measurements were mostly performed at 35 °C. For one brine solution, we verified that the usual temperature relationship was still valid up to 100 °C.

Experimental Method

The variations of viscosity η and conductivity κ were deduced from the measurements of the variations of pressure drop dP when flowing CO₂-saturated solutions across a porous medium and the measurements of the variations of resistance R of this porous media (Figure 1). From Darcy's and Ohm's laws, we have

$$\eta = \frac{SK}{LQ}dP \quad (1)$$

$$\kappa = \frac{1}{f_{\text{cell}}R} \quad (2)$$

where L and S are the length and surface area, respectively, of the porous medium, Q is the flow rate, K is the permeability, and f_{cell} is a geometric cell factor [m]. If all of these factors are kept constant, then the variations of dP and R can be used to characterize the variations of viscosity and conductivity. The resistance R essentially depends on the porosity, whereas the permeability essentially depends on the connections between pores.

A porous medium was specifically designed to have enough contrast in pressure drop variations (i.e., 0.1 MPa) and a moderate resistance (i.e., between (0.1 and 1) k Ω). It is a porous alumina ceramic (custom design by Société des Céramiques Techniques, France) of permeability $2 \cdot 10^{-16}$ m² and porosity 15 % (diameter, 40 mm; length, 30 mm). The porous ceramic sample also has the advantage of not being altered by acidic solutions as well as being weakly sensitive to stress.

The resistance of the porous media was measured using a set of six electrodes located radially around the sample (Figure 1); two pairs of large electrodes are used to inject the current (500 mV, 1 kHz), and the small electrode pair is used to measure the voltage drop. The electrodes are molded in a Viton sleeve, which is also used to apply a confining pressure to the sample. The electrodes are connected to an impedance meter (Agilent 4263), and the resistance is determined from the real part of the measured complex impedance. (The imaginary part is always small and can be used as a quality control of the measurements.) Therefore, hydraulic flow and electric current injection are separated and do not interact with each other.

* Corresponding author. E-mail: marc.fleury@ifp.fr. Fax: 33 1 47 52 70 72.

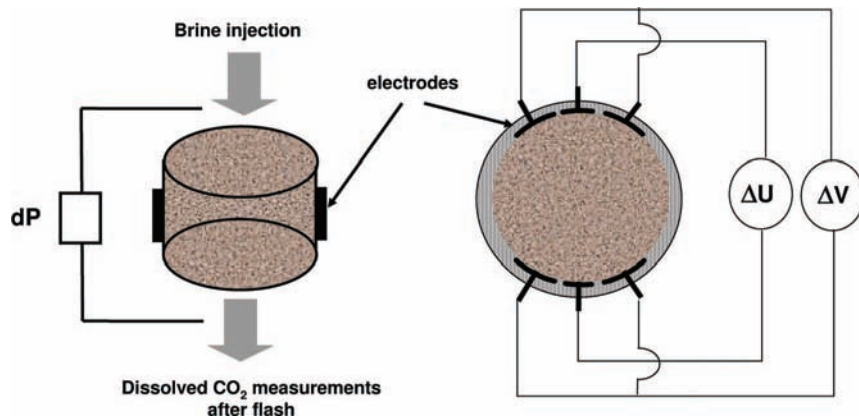


Figure 1. Schematic of the experimental setup for measuring viscosity and conductivity variations of electrolyte solutions containing dissolved CO_2 . The variation of pressure drop dP indicates the variation of viscosity at a constant flow rate. The variation of resistance R indicates the variation of conductivity; using a four-input impedance meter, ΔV is the applied voltage (500 mV, 1 kHz) and ΔU is the measured voltage. From the measured current I circulating in the system as a result of the applied voltage ΔV , we obtain $R = \Delta V/I$. The characteristics of the porous media are: permeability, $2 \cdot 10^{-16} \text{ m}^2$; length, 30 mm; diameter, 40 mm.

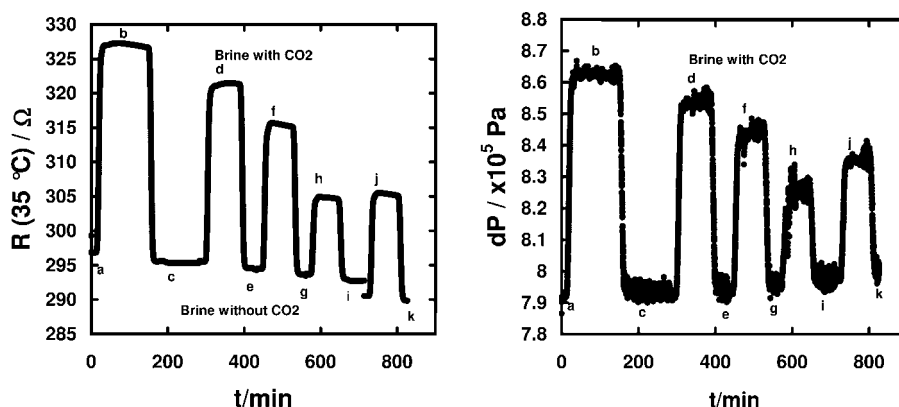


Figure 2. Compilation of different experiments to show the measured variation of resistance R and pressure drop dP for different amounts of dissolved CO_2 ($C_{\text{NaCl}} = 20 \text{ g} \cdot \text{L}^{-1}$). (a,c,e,g,i,k) Reference resistance and pressure drop when flooding with brine alone. (b,d,f,h,j): Resistance and pressure drop when flooding with brine containing dissolved CO_2 . For the last experiment, steps j and k, a small change of porosity may have occurred, therefore modifying the baseline.

Table 1. Accuracy of Measurements

temperature/ $^{\circ}\text{C}$	± 0.1
pressure drop/Pa	± 30
resistance/ Ω	± 0.1
salinity/ $\text{g} \cdot \text{L}^{-1}$	± 0.01
gas volume/L	$\pm 2 \cdot 10^{-4}$

The aqueous NaCl solutions were prepared using deionized water. For a given amount of CO_2 to dissolve, the solutions were placed in a high-pressure Hastelloy container filled at midlevel. Then, CO_2 was injected at the top, and the pressure was imposed at a value varying from 1.0 MPa up to 8.0 MPa to obtain variable amounts of dissolved CO_2 in the brine. To ensure thermodynamic equilibrium, the container was agitated several times. Then, the excess CO_2 was removed, the pressure was increased up to 8.5 MPa (for all experiments), and the solutions were injected through the porous media. To obtain a sealing between the sample and the sleeve, the confining pressure was fixed at 13.5 MPa for all experiments, and the temperature of the flooding cell was fixed at 35 $^{\circ}\text{C}$ (in a temperature-regulated oven), except for the measurements performed at variable temperature described later. Because the solutions were prepared at variable room temperature, the exact amount of dissolved CO_2 was measured after the resistance and pressure drop measurements. This was performed for each experiment on five liquid samples using volumetric brine and gas measurements after a flash and separation at ambient

pressure and temperature. The conversion from gas volume to mole fraction x_{CO_2} takes into account the measured temperature.

The procedure for both resistance and pressure drop measurements is as follows. The brine without CO_2 is first injected at a constant low flow rate of $1 \text{ cm}^3 \cdot \text{h}^{-1}$ through the porous ceramic to determine a reference resistance and pressure drop (step a in Figure 2). Then, the brine with dissolved CO_2 is injected and the variation of resistance and pressure drop is recorded (step b in Figure 2). Finally, the initial brine is injected again to verify that no modification of the porous ceramic occurred during the CO_2 flooding (step c in Figure 2). This procedure is repeated for every experiment when varying the dissolved CO_2 mole fraction. Because of the appropriate choice of the porous ceramic in terms of both permeability and porosity, the variations of resistance and pressure drop are easily measured using standard equipment (up to 20 Ω for R and up to $7 \cdot 10^4$ Pa for dP). The source of uncertainty is mostly due to the baseline fluctuations, a result of the slight modifications of the porous media. For both resistance and pressure drop, the fluctuations of the baseline before and after CO_2 flooding in addition to standard measurement uncertainties (Table 1) were used to calculate error bars (Table 2) for conductivity and viscosity variations.

The measurements at variable temperatures were performed using a continuous increase in the oven temperature while keeping the pore and confining pressures constant. The tem-

Table 2. Relative Variation of Conductivity and Viscosity Deduced from the Relative Variation of Resistance and Pressure Drop as a Function of CO₂ Mole Fraction x_{CO_2} and NaCl Salt Concentration C_{NaCl} at 35 °C and 8.5 MPa

C_{NaCl} g·L ⁻¹	x_{CO_2}	\pm^a	$-\Delta\kappa/\kappa$	\pm^a	$\Delta\eta/\eta$	\pm^a
20	0.0025	0.0003	0.013	0.001	0.012	0.004
20	0.0032	0.0003	0.015	0.001	0.015	0.004
20	0.0045	0.0007	0.024	0.002	0.023	0.005
20	0.0068	0.0003	0.057	0.001	0.034	0.003
20	0.0073	0.0005	0.039	0.001	0.036	0.005
20	0.0081	0.0004	0.041	0.001	0.038	0.005
20	0.0091	0.0004	0.052	0.001	0.046	0.004
20	0.0095	0.0002	0.053	0.001	0.049	0.004
20	0.0104	0.0006	0.071	0.001	0.051	0.002
20	0.0107	0.0007	0.069	0.002	0.053	0.010
20	0.0107	0.0006	0.065	0.001	0.056	0.004
20	0.0116	0.0010	0.077	0.001	0.054	0.004
20	0.0128	0.0006	0.073	0.001	0.062	0.004
20	0.0131	0.0008	0.075	0.001	0.065	0.003
20	0.0132	0.0007	0.085	0.001	0.066	0.004
20	0.0157	0.0004	0.089	0.001	0.076	0.004
20	0.0176	0.0008	0.105	0.001	0.088	0.003
80	0.0024	0.0002	0.015	0.001	0.009	0.003
80	0.0054	0.0003	0.033	0.001	0.024	0.004
80	0.0066	0.0003	0.041	0.001	0.029	0.003
80	0.0081	0.0004	0.049	0.002	0.037	0.004
80	0.0101	0.0004	0.063	0.001	0.045	0.004
80	0.0108	0.0006	0.068	0.001	0.055	0.003
80	0.0115	0.0012	0.076	0.006	0.052	0.020
80	0.0142	0.0009	0.089	0.001	0.068	0.004
80	0.0147	0.0013	0.094	0.002	0.075	0.008
160	0.0046	0.0004	0.026	0.001	0.046	0.033
160	0.0070	0.0007	0.039	0.002	0.024	0.011
160	0.0089	0.0006	0.047	0.002	0.044	0.005
160	0.0103	0.0011	0.060	0.001	0.069	0.009

^a \pm refers to the uncertainties estimated for each quantity in the previous column.

perature was measured close to the sample inside the flooding cell, and the temperature increase ((1 to 3) °C·h⁻¹) was tuned such as to obtain an insignificant temperature difference between the sample and the probe. This is checked by a comparison of the evolution of the temperature and the resistance when the temperature increase is suddenly stopped.

Results

The measured variation of resistance and pressure drop at 35 °C for three salinities representative of the range that can be found in saline aquifers or oil reservoirs is first presented. Then, the effect of temperature on one salinity is described.

Effect of Dissolved CO₂ on Conductivity and Viscosity at 35 °C. A linear relationship can be observed between the relative variation of resistance and the measured mole fraction x_{CO_2} of dissolved CO₂. Therefore, we can deduce the following relationship for conductivity independently of salinity (regression coefficient 0.99, Figure 3)

$$\frac{\Delta\kappa}{\kappa} = -6.0x_{\text{CO}_2} \quad (3)$$

Similarly, for viscosity, the relative variation of the differential pressure is also linearly related to the amount of dissolved CO₂, and we deduce the following relationship (regression coefficient 0.97, Figure 4)

$$\frac{\Delta\eta}{\eta} = 4.65x_{\text{CO}_2} \quad (4)$$

For comparison, we plotted a few data points from the work of Bando et al.² They are in agreement with our observations. The

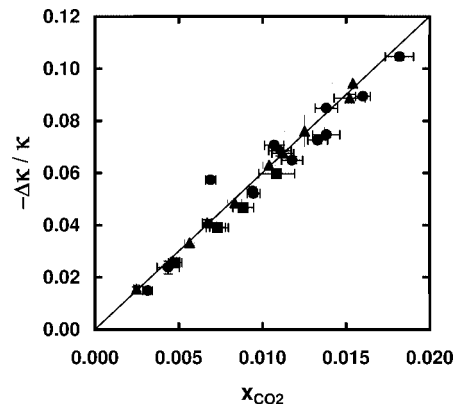


Figure 3. Relative variation of conductivity κ at 35 °C for three salinities C_{NaCl} : ●, 20 g·L⁻¹; ▲, 80 g·L⁻¹; ■, 160 g·L⁻¹; —, best fit eq 3.

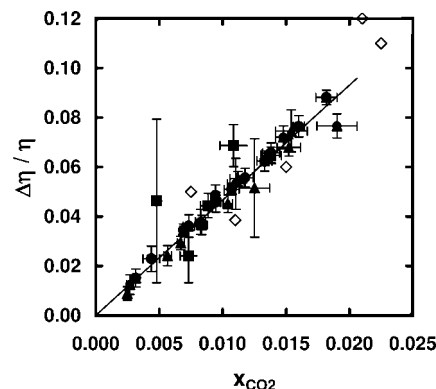


Figure 4. Relative variation of viscosity η for three salinities C_{NaCl} at 35 °C: ●, 20 g·L⁻¹; ▲, 80 g·L⁻¹; ■, 160 g·L⁻¹; ◇, ref 2; —, best fit eq 4.

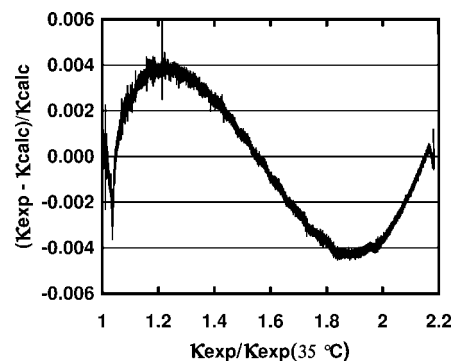


Figure 5. Deviation of measured conductivity κ_{exp} from calculated resistance κ_{calc} using eqs 6 and 2 without dissolved CO₂ ($C_{\text{NaCl}} = 20$ g·L⁻¹, $x_{\text{CO}_2} = 0$, pressure 8.5 MPa). The temperature was varied continuously between (35 and 100) °C.

measured variations of conductivity and viscosity are gathered in Table 2.

Effect of Temperature. For resistivity, a temperature dependence that is routinely used by engineers is known as the Arps empirical law³

$$\kappa_s(T) = \kappa_s(T_0) \frac{T/^\circ\text{C} + C_A}{T_0/^\circ\text{C} + C_A} \quad \text{where } C_A = 21.5 \text{ }^\circ\text{C} \quad (5)$$

The constant C_A may vary slightly from one study to another. In our experience, the above relationship is quite accurate in the range of temperature that is of practical interest in petroleum applications (from (20 to 150) °C), in particular when different ions are considered. For very high salinities (150 g·L⁻¹ and

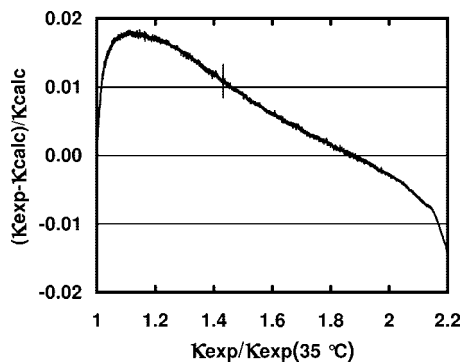


Figure 6. Deviation of measured conductivity κ_{exp} from calculated conductivity κ_{calc} using eqs 6 and 2 with dissolved CO_2 ($C_{\text{NaCl}} = 20 \text{ g}\cdot\text{L}^{-1}$, $x_{\text{CO}_2} = 0.011$, pressure 8.5 MPa). The temperature was varied continuously between (35 and 100) °C. The constant C_A , which was determined for the case without CO_2 , was used in the Arps model.

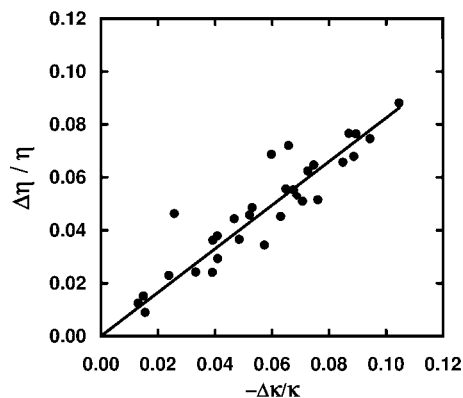


Figure 7. Cross plot of the relative variations of viscosity and conductivity. From data shown in Figures 3 and 4. —, best fit eq 10.

above), the conversion to NaCl equivalent and the use of NaCl tabulated conductivity values may be inaccurate, depending on salt composition. However, the Arps relationship still holds.

We made a comparative study of the temperature dependence with and without dissolved CO_2 for the $20 \text{ g}\cdot\text{L}^{-1}$ NaCl solution. Without CO_2 (Figure 5) and with CO_2 (Figure 6), the data can be fitted with the following

$$\kappa_s(T) = \kappa_s(T_0) \frac{T/^\circ\text{C} + 19.5}{T_0/^\circ\text{C} + 19.5}, \quad 35^\circ\text{C} < T < 100^\circ\text{C} \quad (6)$$

With dissolved CO_2 , the fit is slightly less accurate than it is without CO_2 . (The largest deviation is 1.9 %.) For viscosity, the same law can be applied because the variations of differential pressure were linearly related to the variation of resistance when the temperature was increased (not shown).

Proposed Model. From the experimental results described above, we can deduce the following relationships that describe the effect of dissolved CO_2 on electrical conductivity κ and viscosity η

$$\kappa_s(x_{\text{CO}_2}, T) = \kappa_s(0, T_0) (1 - 6.0x_{\text{CO}_2}) \left(\frac{T/^\circ\text{C} + 19.5}{T_0/^\circ\text{C} + 19.5} \right) \quad (7)$$

$$\eta_s(x_{\text{CO}_2}, T) = \eta_s(0, T_0) (1 + 4.65x_{\text{CO}_2}) \left(\frac{T/^\circ\text{C} + 19.5}{T_0/^\circ\text{C} + 19.5} \right) \quad (8)$$

where the subscript S is used for salinity. These relationships have been established for three NaCl solutions of concentrations (20, 80, and 160) $\text{g}\cdot\text{L}^{-1}$ NaCl ((0.342, 1.369, and 2.738) $\text{mol}\cdot\text{L}^{-1}$, respectively). The temperature dependence has been established in the range of (35 to 100) °C. The mole fraction

x_{CO_2} has been varied up to 0.02, and the measurements have been performed at 8.5 MPa. For viscosity, our temperature dependence yields a smaller decrease than that observed by Bando et al.² For example, from (30 to 60) °C, these authors measured a decrease by a factor of 2.0, whereas we measured a decrease by a factor of 1.8. Our formulation of the viscosity variation also implies that the effect of dissolved CO_2 is not temperature dependent. Using reference values in the absence of CO_2 , we can accurately calculate the conductivity and viscosity. The conductivity of NaCl solutions can be measured or calculated at 25 °C from the following formulas⁴

$$\frac{\kappa_s(0, 25^\circ\text{C})}{(\text{S/m})} = 0.942203 + 0.8889 \log_{10}(C/\text{mol}\cdot\text{L}^{-1}) - 0.0272398 [\log_{10}(C/\text{mol}\cdot\text{L}^{-1})]^2 - 0.00225682 \cdot [\log_{10}(C/\text{mol}\cdot\text{L}^{-1})]^3 + 0.0000146605 \cdot [\log_{10}(C/\text{mol}\cdot\text{L}^{-1})]^4 \quad (9)$$

For viscosity, the model and data collected by Kestin et al.⁵ can be used as references for NaCl solutions as a function of temperature, pressure, and salinity.

Discussion

The two independent measurements of resistivity and viscosity show the same trend: a linear relationship with the mole fraction of dissolved CO_2 . The close link between conductivity and viscosity is expected. Indeed, the conductivity is due to the motions of ions in the solution. For a given ion of radius r , the electric force is balanced by the hydrodynamic drag force, as given by Stoke's law. Therefore, in theory, conductivity and viscosity are inversely proportional according to

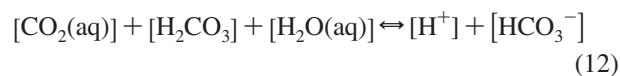
$$\kappa \cdot \eta = \frac{C_w}{r} \quad (10)$$

which is known as the Walden's product. (C_w is a constant. See Smedley⁶ and reference therein.) Therefore, a small relative variation of conductivity should be compensated by the same relative variation of viscosity. A cross plot of the variation of conductivity and viscosity (Figure 7) indicates that this is not exactly true. The relative variation of viscosity is slightly larger than the relative variation of conductivity.

$$\frac{\Delta\eta}{\eta} = -1.3 \frac{\Delta\kappa}{\kappa} \quad (11)$$

However, it is well known that the Walden's product is an oversimplification and may be valid in a very dilute system without ion interactions. Also note that the increase in viscosity cannot be due to only the increase in density that is much smaller¹ (maximum 1 %).

When CO_2 is dissolved, additional ions are formed according to the following reaction



Other subspecies are also formed, but they can be neglected here. Therefore, we can expect an increase in conductivity. However, a simple dissociation calculation show that at the lowest possible pH (about 3) the H^+ concentration will be about $10^{-3} \text{ mol}\cdot\text{L}^{-1}$ (by definition), whereas the NaCl concentration will be more than 100 times larger ($0.342 \text{ mol}\cdot\text{L}^{-1}$ for the lowest salinity considered here). Therefore, the contribution of these additional ions is negligible for the considered salinities,

and the conductivity is dominated by ions originating from the dissolved salts.

The temperature dependence of viscosity is usually expressed with good accuracy as a modified Arrhenius law of the form⁷

$$\eta = \eta_C \cdot \exp\left(\frac{C_\eta}{T - T_c}\right) \quad (13)$$

where C_η is a constant and η_C is a prefactor. Such laws are applicable to crude oils in a wider range of temperature than that considered in this study. The empirical proposed model that originated from the Arps law does not contradict the above equation and has the advantage of being accurate with only one adjustable parameter. From our experience, the Arps law is accurate for a wide range of salt composition and total salinity in the temperature range of (20 to 120) °C. Therefore, it should also be valid for viscosity.

Conclusions

The effect of dissolved CO₂ on the resistivity and viscosity of aqueous NaCl solutions is small and can be modeled by the use of a simple linear function that involves the mole fraction. The experiments have been performed on three NaCl solutions covering the range of salinity that is usually encountered in potential CO₂ storage geological formations. We show that the variation of conductivity and viscosity are proportional to the mole fraction of dissolved CO₂ at a constant temperature of 35 °C. The relative variation of viscosity is slightly larger than the relative variation of conductivity. For viscosity, our data are in

agreement with previous observations. For one brine, the variations of conductivity and viscosity with and without dissolved CO₂ were determined up to 100 °C and fitted with the Arps empirical law using the same fitting coefficient. Finally, we propose a simple model to take into account the effect of both dissolved CO₂ and temperature.

Literature Cited

- (1) Teng, H.; Yamasaki, A.; Chun, M.; Lee, H. Solubility of liquid CO₂ in water at temperatures from 278 to 293 K and pressures from 6.44 to 29.49 MPa and densities of the corresponding aqueous solutions. *J. Chem. Thermodyn.* **1997**, *29*, 1301–1310.
- (2) Bando, S.; Takemura, F.; Nishio, M.; Hihara, E.; Akai, M. Viscosity of aqueous NaCl solutions with dissolved CO₂ at (30 to 60) °C and (10 to 20) MPa. *J. Chem. Eng. Data* **2004**, *49*, 1328–1332.
- (3) Arps, J. J. The effect of temperature on the density and electrical resistivity of sodium chloride solutions. *Trans. Am. Inst. Min., Metall. Pet. Eng.* **1953**, *198*, 327–330.
- (4) Worthington, A. E.; Hedges, J. H.; Pallat, N. Guidelines for preparation of brine and determination of brine resistivity for use in electrical resistivity measurements. *Log Analyst* **1990**, *31*, 20–28.
- (5) Kestin, J.; Khalifa, E.; Correia, R. J. Tables of the dynamic and kinematic viscosity of aqueous NaCl solutions in the temperature range 20–150 °C and the pressure range 0.1–35 MPa. *J. Phys. Chem. Ref. Data* **1981**, *10*, 71–87.
- (6) Smedley, S. I. *The Interpretation of Ionic Conductivity in Liquids*; Plenum Press: New York, 1980.
- (7) Beggs, H. D.; Robinson, J. R. Estimating the viscosity of crude oil system. *J. Pet. Technol.* **1975**, *27*, 1140–1141.

Received for review April 16, 2008. Accepted September 18, 2008.

JE8002628